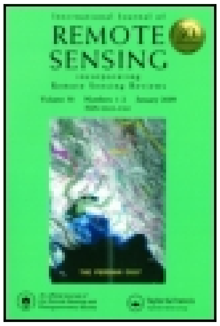

International Journal of Remote Sensing
Publication details, including instructions for authors and subscription information:
http://www.tandfonline.com/loi/tres20

A satellite case study of a katabatic surge along the Transantarctic Mountains

D. H. BROMWICH [a]

[a] Byrd Polar Research Center, The Ohio State Universit, Columbus, Ohio, 43210, U.S.A

Available online: 17 Apr 2007

To cite this article: D. H. BROMWICH (1992): A satellite case study of a katabatic surge along the Transantarctic Mountains, International Journal of Remote Sensing, 13:1, 55-66

To link to this article: http://dx.doi.org/10.1080/01431169208904025

INT. J. REMOTE SENSING, 1992, VOL. 13, NO. 1, 55-66

A satellite case study of a katabatic surge along the Transantarctic Mountains

D. H. BROMWICH

Byrd Polar Research Center, The Ohio State University, Columbus, Ohio 43210, U.S.A.

Abstract. A low-light visible/near-infra-red satellite image of the Ross Ice Shelf area at 1510 UTC on 1 November 1986 showed a cloud-free region along the Transantarctic Mountains from the Liv Glacier northward. The corresponding thermal infra-red image indicated that the clear area was a katabatic air mass, fed by katabatic winds blowing from the main glacier valleys that dissect the Transantarctic Mountains. The cloud-free area broadened to the north and its western edge passed just to the east of Minna Bluff. The katabatic air mass crossed the edge of the Ross Ice Shelf, extended about 350 km offshore and developed cloud streets. Thus, this katabatic airstream appeared to propagate horizontally for over 1300 km. Analyses are presented of its association with the regional atmospheric circulation, of its time evolution and of its probable impact on the sea ice cover over the Ross Sea. Aspects of the governing dynamics are discussed.

1. Introduction

Katabatic winds blow with great frequency down the coastal slopes of Antarctica. Until recently it was widely believed that all katabatic winds usually dissipate within 10-20 km past the foot of the terrain slope (for example, Schwerdtfeger 1970), where the downslope buoyancy force goes to zero. Abundant evidence demonstrates that this general result does not apply in the Ross-Sea/Ross-Ice-Shelf sector of the Antarctic. At Terra Nova Bay, for example, intense winter katabatic winds propagate 34 km across the flat Nansen Ice Sheet with great frequency (Bromwich 1989 a). Direct wind measurements show that, at times, katabatic airflows from Terra Nova Bay can blow for hundreds of kilometres across the ice-covered Ross Sea (Bromwich 1986, Parish and Bromwich 1989).

Thermal infra-red satellite images are a valuable tool for the study of katabatic winds over the Ross Ice Shelf (D'Aguanno 1986). Prominent warm signatures of katabatic airflows are climatological features over the shelf and are apparently caused by intense vertical mixing and drift-snow transport within stable boundary layers (Bromwich 1989 b, Parish and Bromwich 1989); the signatures closely match surface wind measurements from automatic weather stations (AWS) (Bromwich 1989 b). Similar to the results outlined above, katabatic wind signatures can extend horizontally for 500 km or more across the Ross Ice Shelf (Stearns and Wendler 1988).

This paper combines conventional weather observations and satellite images to describe and understand the apparent horizontal propagation of a katabatic air mass along the Transantarctic Mountains for distances in excess of 1000 km. Section 2 describes the katabatic wind from the perspective of satellite images. This is followed by a surface and mid-tropospheric description of the regional atmospheric circulation. Section 4 outlines the probable impact on sea ice of the offshore airflow. The final section offers some thoughts on the governing dynamics.

2. AVHRR depiction

A visible/near-infra-red satellite image (from National Oceanic and Atmospheric Administration's NOAA-10 Advanced Very High Resolution Radiometer (AVHRR) Channel 2) of the Ross Ice Shelf taken in the early morning at the beginning of November 1986 (15 10 UTC on 1 November 1986, 03 10 local time on 2 November) showed a cloud-free zone along the Transantarctic Mountains from Liv Glacier northward (see figure 1). The clear area broadened to the north, passed eastward around Minna Bluff, and developed cloud streets out over the sea ice to the north of the Ross Ice Shelf. The accompanying thermal infra-red image (AVHRR Channel 4) showed signatures of katabatic winds blowing from numerous glaciers into the cloud-free zone; it is likely that the dryness of the subsided katabatic air dissolved the low clouds adjacent to the foot of the mountains. The glacier valleys provide pathways for cold air to descend through the Transantarctic Mountains from the high polar plateau (elevation >2000 m asl) to the flat ice shelf, whose height above sea level averages 60 m. The presence of these signatures in the clear zone, together with its northward broadening, suggest that it is a boundary-layer air mass formed by katabatic drainage. The complete eastward deflection of the airstream by the 600–1000-m-high obstacle of Minna Bluff is consistent with the airstream being stably stratified, possessing moderate momentum and being a few hundred metres deep (based on the Froude-number discussion presented by O'Connor and Bromwich 1988)—in line with the characteristics expected for a katabatic air mass blowing horizontally along the Transantarctic Mountains.

Figure 2 shows a blow-up of the satellite image centred on Beardmore Glacier (see figure 1 for location). The visible/near-infra-red image (figure 2 (*a*)) shows the polar plateau in the lower left with the east-facing peaks of the Transantarctic Mountains being highlighted by the rays of the early morning sun which approach from the lower right. The clear slot over the shelf parallels the mountains. The top right half of the image is covered by low clouds associated with the cyclone discussed in section 3. Simultaneous surface observations of wind, temperature and pressure are plotted from AWS 11 and 08 and demonstrate that the winds are light at 2·5 and 5 m s^{-1}, respectively. The thermal infra-red image (figure 2 (*b*)) reveals dark (warm) katabatic wind signatures from the polar plateau, down many glacier valleys and out into the clear area over the Ross Ice Shelf. The most prominent signature is associated with Nimrod Glacier. The signatures typically lose their definition a short distance out over the shelf ($\leq$60 km); several turn left and merge into the streaked zone that generally parallels the mountains. The lack of distinctive surface wind signatures in the thermal infra-red over most of the ice shelf is consistent with the light wind speed (2·5 m s^{-1}) recorded at AWS 11. The wind direction at AWS 11 cuts across the edge of the cloud deck (figure 2 (*a*)), indicating that this site is in the transition zone between the katabatic airmass along the mountains and the cyclonically controlled circulation to the northeast.

The prominent lines in figure 2 (*b*) that emerge from Beardmore Glacier and the next glacier to the northwest, Lennox-King, are believed to be ice-flow features and arise because of the effect of slight variations in surface topography on viewing angle and, thus, on the snow-surface emissivity (G. Casassa, personal communication, 1990). Some of these glaciological features are also evident in the visible/near-infra-red image (figure 2 (*a*)). The relative contributions of glaciological and meteorological effects to the thermal infra-red streaks (figure 2 (*b*)) in the clear zone (figure 2 (*a*)) are not completely understood and require further study.

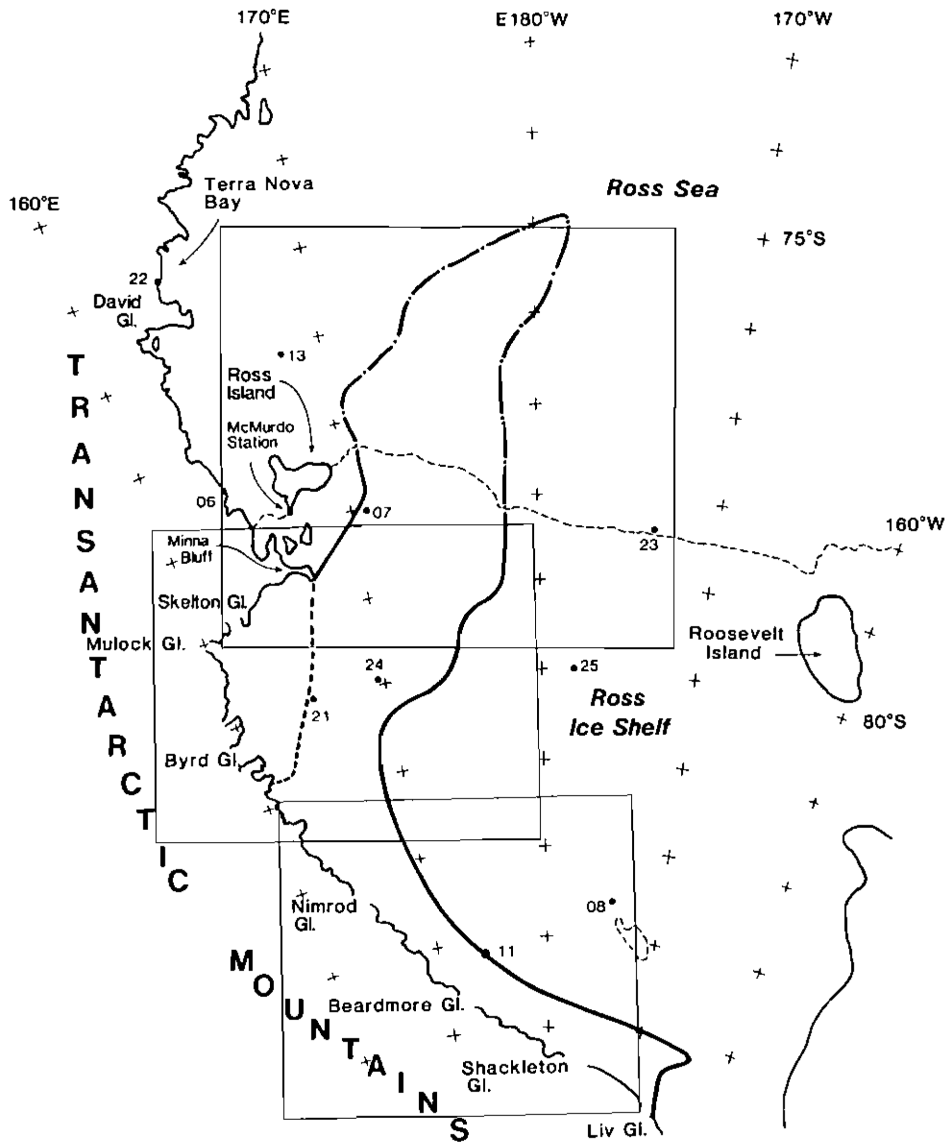

Figure 1. Regional location map. Solid line outlines the cloud-free zone along the Transantarctic Mountains shown on an AVHRR visible/near-infra-red image at 15 10 UTC on 1 November 1986. The dashed line between Minna Bluff and Byrd Glacier marks the eastern boundary of a patchy, thin middle-level cloud band. The dot-dash line encloses the cloud streets over the Ross Sea. The boxes denote areas covered by figures 2-4. The dots with adjacent bold numbers are AWS sites.

(a)

(b)

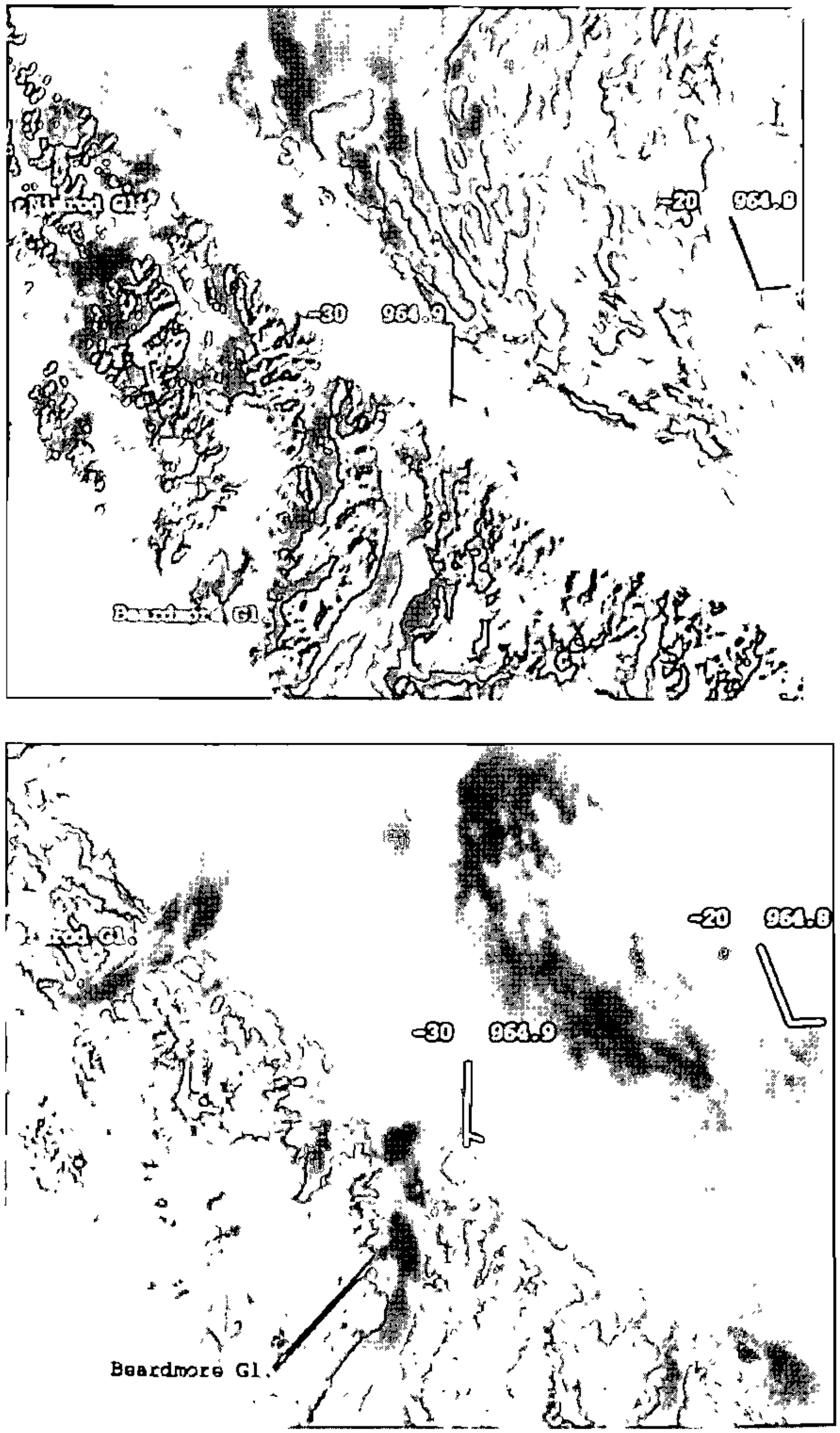

Figure 2. Close-up centred near Beardmore Glacier (see figure 1 for location) of AVHRR imagery at 15 10 UTC on 1 November 1986—(*a*) visible/near-infra-red (Channel 2), (*b*) thermal infra-red (Channel 4). The plotted data are simultaneous AWS observations (AWS 11 centre, AWS 08 to the right), with air temperature in degrees Celcius on the left and *station* air pressure in hectopascals to the right. The direction from which the wind blows is given by orientation of the line drawn to the AWS location, with the attached short barb denoting a wind speed of $2 \cdot 5 \mathrm{~m} \mathrm{~s}^{-1}$ and the long barb $5 \mathrm{~m} \mathrm{~s}^{-1}$.

Another examination of the adjustment of katabatic airstreams to airflow over the Ross Ice Shelf is provided by figure 3. This is a thermal image centred further north, near Byrd Glacier. To facilitate feature identification the temperature display is reversed from that of figure 2 (*b*), with the warmest temperatures appearing as the lightest tones. The bright (warm) katabatic streams from Skelton, Mulock and, particularly, Byrd glaciers (to the left) merge and are deflected around the eastern edge of Minna Bluff (top left of centre); a limited area of thin middle cloud partially obscures the confluence of the streams from Mulock and Byrd glaciers. Marked streaks emerge from the end of Byrd Glacier's katabatic wind signature and may, as before, reflect a combination of glaciological and meteorological effects. AWS 24 is outside of the domain of the merged katabatic airstreams from Skelton, Mulock and Byrd glaciers, but its wind direction nearly parallels the orientation of a thermal streak that originates to the south. Notice that figure 3 gives the impression, from the cold area (dark) at bottom left, of merging katabatic air masses from southern and northern sources. Warm low cloud (bright) associated with the cyclone covers the right side of the image.

After the katabatic air mass crosses from the ice shelf to the Ross Sea, cloud streets quickly develop in the boundary layer, presumably due to the condensation of moisture that evaporated from the partially ice-covered Ross Sea. Figure 4 is a visible/near-infra-red blow-up centred over the northwestern part of the Ross Ice Shelf. Cloud streets, aligned parallel to the surface wind direction, can be seen

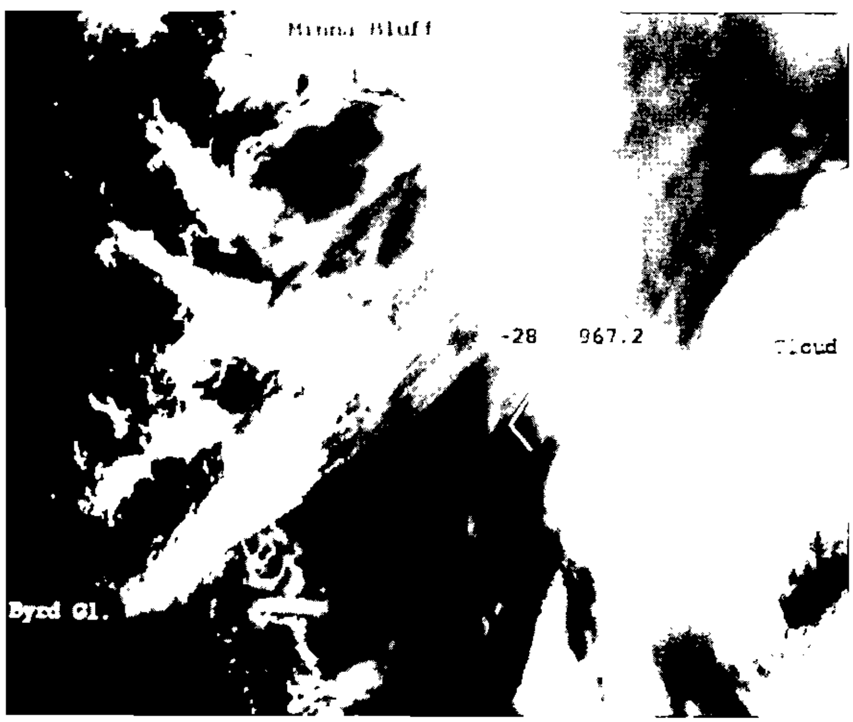

Figure 3. Same as figure 2 (*b*), but centred near Byrd Glacier and with a reversed temperature display; here, the warmest temperatures are the lightest tones. Observations for AWS 24 are given.

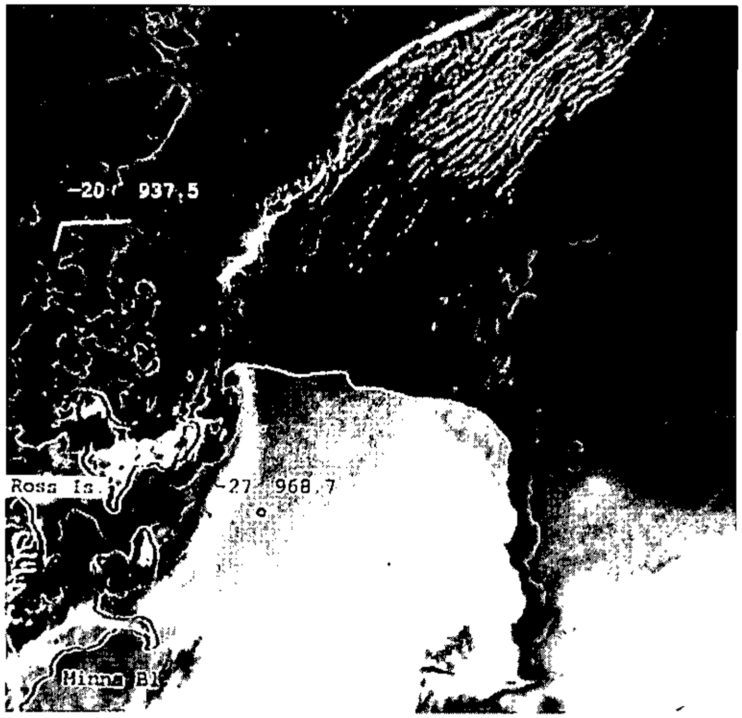

Figure 4. Same as figure 2(*a*), but centred over the northwestern part of the Ross Ice Shelf. No wind observations are available for AWS 07, which is located to the northeast of Minna Bluff and is embedded within the katabatic air mass. The observations further north are for AWS 13.

immediately to the north of the sharply defined edge of the shelf. Rays from the sun, which is near the horizon, approach from the lower right and illuminate Minna Bluff, Ross Island and the edge of the low cloud along the western side of the cloud-street zone. The cloud edge to the east of the cloud streets casts a shadow on the surface.

3. Regional atmospheric circulation

Surface observations from the array of satellite-transmitting AWS over the Ross-Sea/Ross-Ice-Shelf area (Sievers *et al.* 1987) can be used to construct the sea-level pressure field at image time. Figure 5 reveals that a well-defined low-pressure trough was situated over the eastern side of the Ross Ice Shelf. Drainage of katabatic air through the Transantarctic Mountains and adjustment to mountain-parallel flow over the shelf takes place in the zone of weak pressure gradients in association with the ridge along the mountains. The eastern boundary of the katabatic air mass approximately coincides with the western edge of the zone of marked pressure gradients. The adjusted katabatic airstream blows northward along the mountains in an approximately geostrophic direction up to the latitude of Byrd Glacier. Further northward, significant cross-isobaric airflow is manifested. Numerical modelling calculations and thermal infra-red satellite imagery suggest that a large katabatic mass transport typically issues from Byrd Glacier (Parish and Bromwich 1987, Bromwich 1989 b). The ageostrophic motions north of Byrd Glacier could be

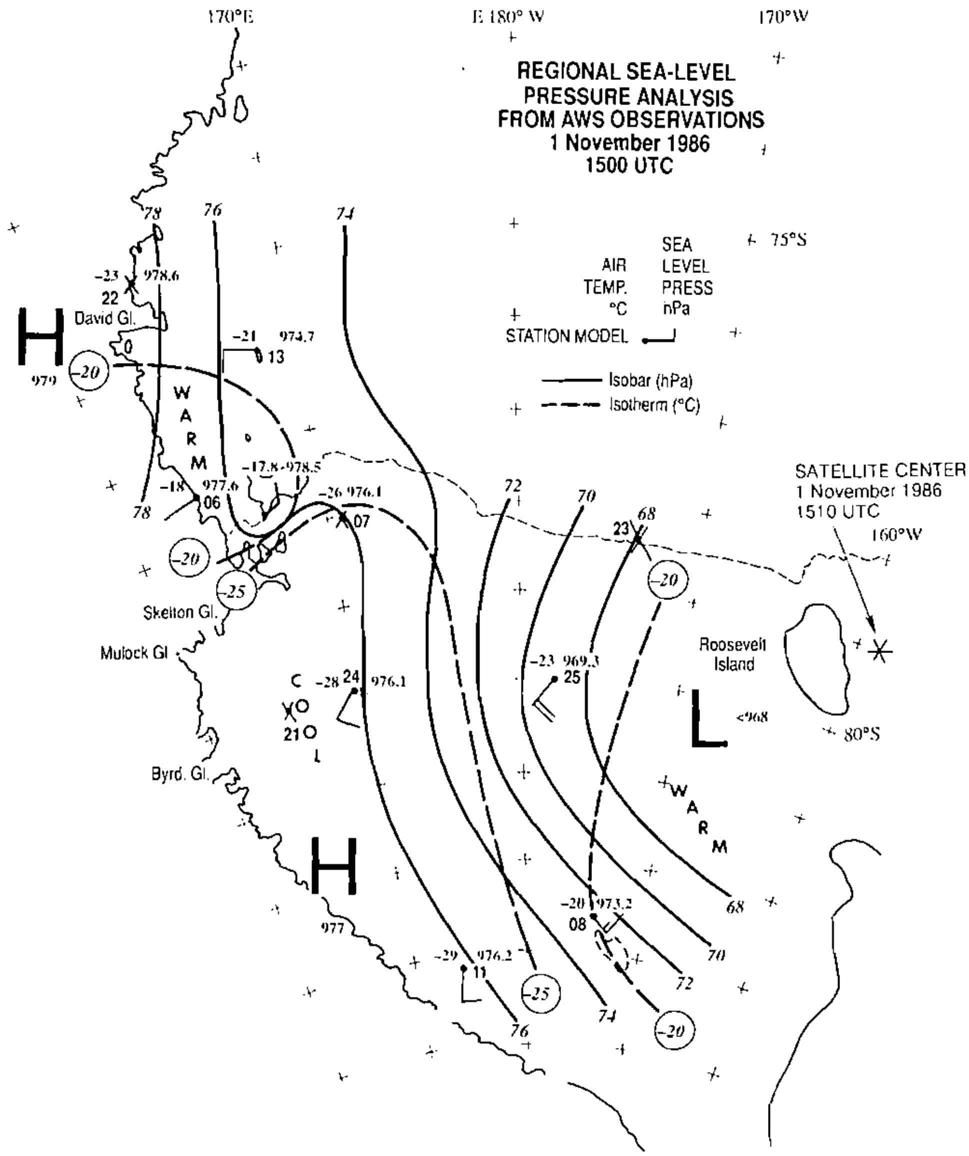

Figure 5. Regional sea-level pressure analysis for 1500 UTC on 1 November 1986 constructed from AWS observations. Solid lines are sea-level isobars in hectopascals (76 = 976 hPa) and dashed lines are surface isotherms in degrees Celcius. The wind vector plotting convention is described in the caption to figure 2; in addition, a direction line without an attached barb indicates a speed of less than 1·3 m s^{-1}. A cross through the AWS location implies either no data at all or no wind observations. The asterisk to the right of Roosevelt Island is the satellite centre. Data used for this analysis differ slightly from those entered in figures 2–4 because of the 10-min time difference.

associated with a deep and vigorous mass transport from the glacier, which also causes eastward deflection of the mountain-parallel airstream originating further to the south. It is notable that down-gradient airflow is also present at AWS 13 (Franklin Island), which is probably caused by intense katabatic mass transport from Terra Nova Bay (for example, Bromwich 1986). The satellite-observed presence of a large polynya in the bay supports the hypothesis of strong katabatic winds (compare Bromwich and Kurtz 1984). The cloud-street-filled katabatic air mass over the Ross Sea appears to be moving in a geostrophic direction; a precise comparison is not possible because the isobar orientations in this area are uncertain.

The temporal evolution of the katabatic surge is summarized by figure 6. Defining the surge in terms of southerly winds at AWS 11 shows that the event started at 1200 UTC on 31 October and ended just after 1800 UTC on 1 November. Thus, the image depictions presented in section 2 represent surge conditions 27 h after onset and about 3 h before its cessation. If the typical speed of adjusted katabatic airflow along the mountains is $5\,\mathrm{m\,s^{-1}}$, then in the 27 h between surge onset and image time the katabatic air could only have travelled about 480 km to the north of Beardmore Glacier—it could not have reached the edge of the Ross Ice Shelf. This suggests that the katabatic air mass over the Ross Sea which is shown by the imagery to contain cloud streets is generated by katabatic drainage from Byrd and adjacent glaciers. The down-gradient katabatic airflow at Franklin Island started at 0600 UTC on 1 November and continued for 24 h.

Consistent with the regional sea-level pressure depiction in figure 5, figure 6 shows that during the surge at AWS 11 the pressure was higher along the mountains than out over the shelf. This was associated with two pressure patterns. During the

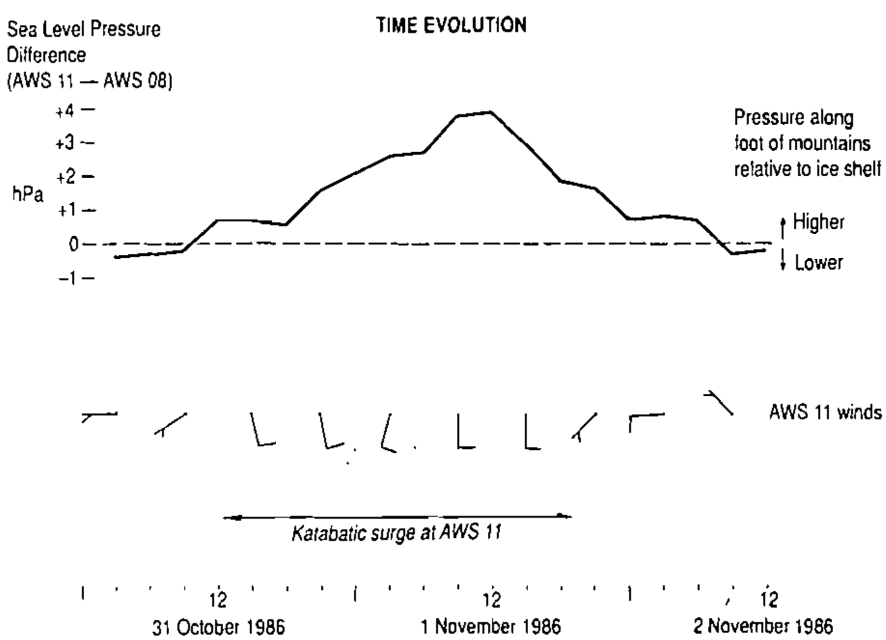

Figure 6. Time evolution of sea-level pressure and surface winds near the foot of Beardmore Glacier. Winds that are shown blowing from the bottom to the top are southerlies.

first 9 h (12 00 UTC to 21 00 UTC on 31 October) the pressure uniformly decreased from a maximum along the mountains to a minimum out over the Ross Sea. An AVHRR image at 17 10 UTC on 31 October showed a subsynoptic-scale low over the Ross Sea near 76° S 160° W. Later images verified that this cyclone was moving slowly southward, and as a result the AWS analyses subsequently resolved a pronounced trough (pressure pattern number 2) over the eastern side of the Ross Ice Shelf which developed around 21 00 UTC on 31 October. The hemispheric sea-level pressure analyses for 00 00 UTC on 1 November prepared by the Australian Bureau of Meteorology, Melbourne, revealed a deep maritime cyclone (central pressure less than 960 hPa) near 70° S 175° W. The subsynoptic low, which was not analysed on the Australian charts, was probably associated with the maritime cyclone further to the north. From 21 00 UTC on 31 October to 18 00 UTC on 1 November (21 h) the regional pressure distribution was nearly identical to that in figure 5. After 18 00 UTC on 1 November the pressure distribution changed rapidly as the subsynoptic-scale cyclone dissipated over the northeastern part of the Ross Ice Shelf, and the surge ended abruptly at AWS 11.

4. Sea-ice impact

A notable characteristic of the Ross Sea is the disintegration of the sea ice cover during the warmer months. West of about the 180° meridian the ice cover disintegrates northward from the Ross Ice Shelf and southward from the Southern Ocean (for example, Zwally *et al.* 1983). This process starts in late October or early November and is complete by early January to mid-January when the entire area is ice-free. To the author's knowledge, little has been written on the precise cause of this northward ice dissipation.

Figure 7 sketches from the weekly Navy-NOAA Joint Ice Center analyses (Naval Polar Oceanography Center 1987) the area of reduced ice concentration along and immediately to the north of the Ross Ice Shelf just before and after the surge event. During this 1-wk interval the area of reduced ice concentration became greatly enlarged to the west of 180°; on the west side of Ross Island, which was sheltered from the katabatic surge by Minna Bluff, there was little change to the sea ice cover. The general shape of the reduced ice concentration area on 6 November is similar to the domain occupied by the cloud-street-filled katabatic air mass of 15 10 UTC 1 November. This suggests a causal link.

It appears that the area of reduced ice concentration was generated by the offshore katabatic winds. Generally rising air temperatures probably did not favour subsequent formation of substantial amounts of new ice in the area with depleted sea ice cover. As a result, this zone would have absorbed much larger amounts of solar radiation than the surrounding areas with more reflective and concentrated sea ice, thus tending to perpetuate the reduced ice concentrations. By contrast, winter conditions favour the rapid filling of such polynya areas by new ice formation (Zwally *et al.* 1985). The zone of reduced ice concentration formed a nucleus for the subsequent northward disintegration of the ice cover. Presumably, similar wind events, northward surface currents and heat stored in the ocean (Jacobs and Comiso 1989) continued the dissipation.

5. Conclusions

This study has outlined a katabatic surge which apparently set the stage for the start of disintegration of the sea ice over the Ross Sea. Similar to other studies of

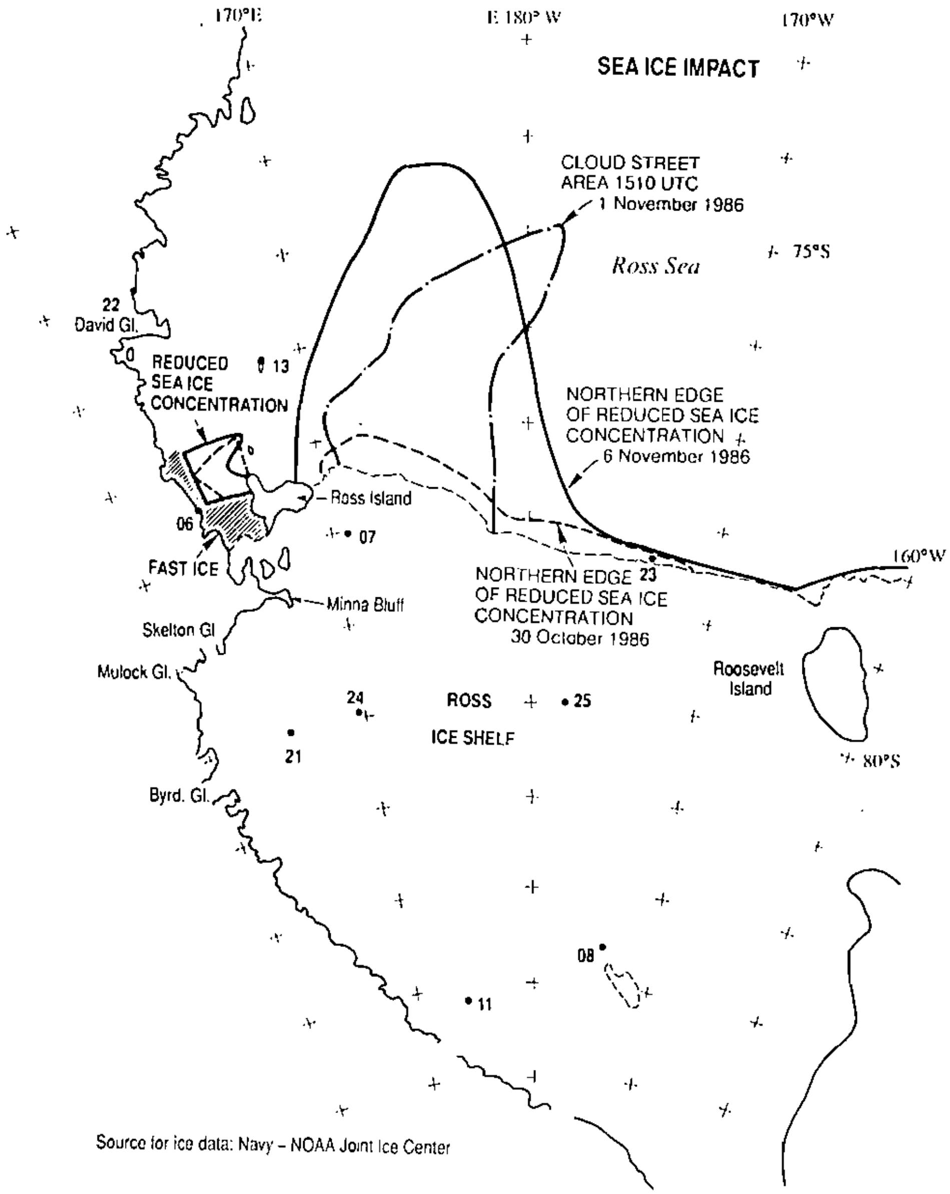

Figure 7. Comparison of cloud street area over the Ross Sea at 1510 UTC on 1 November 1986 with sea-ice analyses before and after the katabatic surge.

marked katabatic drainage onto the Ross Ice Shelf, this was associated with the regional presence of a large cyclone (Breckenridge 1985, Bromwich 1989 b). In this case, however, upper winds did not assist the downslope flow, being from the north and northeast at the 500 hPa level throughout the event (established from Australian 500-hPa hemispheric analyses and soundings from McMurdo Station on Ross Island). In the ridge zone of weak pressure gradients along the mountains, katabatic winds from many glaciers turned left in a pseudo-inertial fashion and adjusted within 60 km from the mountain base to a geostrophic orientation. Northward advection parallel to the mountains was then supported by the regional pressure field. Ageostrophic (cross-isobaric) motions for hundreds of kilometres beyond the foot of the terrain slope appeared to be associated with airflow from glaciers where the katabatic mass transport from the polar plateau is concentrated (Byrd Glacier and Terra Nova Bay). Eventually, these enhanced katabatic airstreams adjusted to, and subsequently followed, a geostrophic orientation.

Several aspects of this work need to be improved. Winter cases should be studied so that better developed katabatic wind signatures are available. Efforts are required so that the glaciological and meteorological contributions to the thermal streaks over the Ross Ice Shelf can be confidently separated. Studies should be concentrated in those years during which the AWS array is more extensive so that the dominant katabatic airstreams are adequately sampled. Finally, further work is needed to isolate the precise causes of sustained periods of katabatic drainage through the Transantarctic Mountains over a meridional distance of about 1300 km; in particular, the limitations imposed on the coastal katabatic winds by the supply of cold air over the polar plateau need to be isolated.

Acknowledgments

This research was supported by National Science Foundation grant DPP-8716339. Mr Robert H. Whritner of the Antarctic Research Centre at Scripps Institution of Oceanography brought this case to the author's attention, and did some preliminary processing of the satellite imagery. The AVHRR data presented in section 2 were recorded by US Navy personnel at McMurdo Station, and were obtained on video cassettes from Mr Whritner, whose activities are funded by NSF grant DPP-8815818. The imagery was processed on a SUN 4 workstation using the TeraScan software supplied by SeaSpace. Collection and distribution of the US AWS data are supported by NSF grant DPP-8818171 to Charles R. Stearns. Stan Jacobs offered some helpful comments on the manuscript. Contribution 708 of the Byrd Polar Research Center.

References

BRECKENRIDGE, C. J., 1985, Foehn events along the Transantarctic Mountains. M.S. thesis, Department of Meteorology, University of Wisconsin-Madison.

BROMWICH, D. H., 1986, Boundary layer meteorology of the western Ross Sea. *Antarctic Journal of the United States*, **21**(5), 237–240.

BROMWICH, D. H., 1989 a, An extraordinary katabatic wind regime at Terra Nova Bay, Antarctica. *Monthly Weather Review*, **117**, 688–695.

BROMWICH, D. H., 1989 b, Satellite analyses of Antarctic katabatic wind behavior. *Bulletin of the American Meteorological Society*, **70**, 738–749.

BROMWICH, D. H., and KURTZ, D. D., 1984, Katabatic wind forcing of the Terra Nova Bay polynya. *Journal of Geophysical Research*, **89**, 3561–3572.

D'AGUANNO, J., 1986, Use of AVHRR data for studying katabatic winds in Antarctica. *International Journal of Remote Sensing*, **7**, 703–713.

JACOBS, S. S., and COMISO, J. C., 1989, Sea ice and oceanic processes on the Ross Sea continental shelf. *Journal of Geophysical Research*, **94**, 18195–18211.

NAVAL POLAR OCEANOGRAPHY CENTER, 1987, *Antarctic Ice Charts 1985–1986* (Washington, DC: Naval Polar Oceanography Center).

O'CONNOR, W. P., and BROMWICH, D. H., 1988, Surface airflow around Windless Bight, Ross Island, Antarctica. *Quarterly Journal of the Royal Meteorological Society*, **114**, 917–938.

PARISH, T. R., and BROMWICH, D. H., 1987, The surface windfield over the Antarctic ice sheets. *Nature*, **328**, 51–54.

PARISH, T. R., and BROMWICH, D. H., 1989, Instrumented aircraft observations of the katabatic wind regime near Terra Nova Bay. *Monthly Weather Review*, **117**, 1570–1585.

SCHWERDTFEGER, W., 1970, The climate of the Antarctic. In *Climates of the Polar Regions* (World Survey of Climatology, Vol. 14), edited by S. Orvig (Amsterdam, London, New York: Elsevier), p. 293.

SIEVERS, M. F., WEIDNER, G. A., and STEARNS, C. R., 1987, Antarctic automatic weather station data for the calendar year 1986, Department of Meteorology, University of Wisconsin-Madison.

STEARNS, C. R., and WENDLER, G., 1988, Research results from Antarctic automatic weather stations. *Reviews of Geophysics*, **26**, 45–61.

ZWALLY, H. J., COMISO, J. C., and GORDON, A. L., 1985, Antarctic offshore leads and polynyas and oceanographic effects. In *Oceanology of the Antarctic Continental Shelf*, Antarctic Research Series, Vol. 43, edited by S. S. Jacobs (Washington, DC: American Geophysical Union).

ZWALLY, H. J., COMISO, J. C., PARKINSON, C. L., CAMPBELL, W. J., CARSEY, F. D., and GLOERSEN, P., 1983, *Antarctic Sea Ice, 1973–1976: Satellite Passive-Microwave Observations*, NASA SP-459 (Washington, DC: National Aeronautics and Space Administration).